



ELSEVIER

SCIENCE @ DIRECT®

PHYSICS LETTERS B

Physics Letters B 591 (2004) 23–41

www.elsevier.com/locate/physletb

Search for contact interactions, large extra dimensions and finite quark radius in ep collisions at HERA

ZEUS Collaboration

S. Chekanov, M. Derrick, D. Krakauer, J.H. Loizides¹, S. Magill, S. Miglioranzi¹,
B. Musgrave, J. Repond, R. Yoshida

Argonne National Laboratory, Argonne, IL 60439-4815, USA⁴⁵

M.C.K. Mattingly

Andrews University, Berrien Springs, MI 49104-0380, USA

P. Antonioli, G. Bari, M. Basile, L. Bellagamba, D. Boscherini, A. Bruni, G. Bruni,
G. Cara Romeo, L. Cifarelli, F. Cindolo, A. Contin, M. Corradi, S. De Pasquale,
P. Giusti, G. Iacobucci, A. Margotti, A. Montanari, R. Nania, F. Palmonari, A. Pesci,
G. Sartorelli, A. Zichichi

University and INFN Bologna, Bologna, Italy³⁶

G. Aghuzumtsyan, D. Bartsch, I. Brock, S. Goers, H. Hartmann, E. Hilger, P. Irrgang,
H.-P. Jakob, O. Kind, U. Meyer, E. Paul², J. Rautenberg, R. Renner, A. Stifutkin,
J. Tandler, K.C. Voss, M. Wang, A. Weber³

Physikalisches Institut der Universität Bonn, Bonn, Germany³³

D.S. Bailey⁴, N.H. Brook, J.E. Cole, G.P. Heath, T. Namsou, S. Robins, M. Wing

H.H. Wills Physics Laboratory, University of Bristol, Bristol, United Kingdom⁴⁴

M. Capua, A. Mastroberardino, M. Schioppa, G. Susinno

Physics Department, Calabria University, and INFN, Cosenza, Italy³⁶

J.Y. Kim, Y.K. Kim, J.H. Lee, I.T. Lim, M.Y. Pac⁵

Chonnam National University, Kwangju, South Korea³⁸

A. Caldwell⁶, M. Helbich, X. Liu, B. Mellado, Y. Ning, S. Paganis, Z. Ren,
W.B. Schmidke, F. Sciulli

Nevis Laboratories, Columbia University, Irvington on Hudson, NY 10027, USA⁴⁶

J. Chwastowski, A. Eskreys, J. Figiel, A. Galas, K. Olkiewicz, P. Stopa, L. Zawiejski

Institute of Nuclear Physics, Cracow, Poland⁴³

L. Adamczyk, T. Bołd, I. Grabowska-Bołd⁷, D. Kisielewska, A.M. Kowal, M. Kowal,
T. Kowalski, M. Przybycień, L. Suszycki, D. Szuba, J. Szuba⁸

Faculty of Physics and Nuclear Techniques, AGH-University of Science and Technology, Cracow, Poland⁴⁷

A. Kotański⁹, W. Słomiński

Department of Physics, Jagellonian University, Cracow, Poland

V. Adler, U. Behrens, I. Bloch, K. Borrás, V. Chiochia, D. Dannheim, G. Drews,
J. Fourletova, U. Fricke, A. Geiser, P. Göttlicher¹⁰, O. Gutsche, T. Haas, W. Hain,
S. Hillert¹¹, B. Kahle, U. Kötz, H. Kowalski¹², G. Kramberger, H. Labes, D. Lelas,
H. Lim, B. Lühr, R. Mankel, I.-A. Melzer-Pellmann, C.N. Nguyen, D. Notz,
A.E. Nuncio-Quiroz, A. Polini, A. Raval, L. Rurua, U. Schneekloth, U. Stösslein,
R. Wichmann¹³, G. Wolf, C. Youngman, W. Zeuner

Deutsches Elektronen-Synchrotron DESY, Hamburg, Germany

S. Schlenstedt

DESY Zeuthen, Zeuthen, Germany

G. Barbagli, E. Gallo, C. Genta, P.G. Pelfer

University and INFN, Florence, Italy³⁶

A. Bamberger, A. Benen, F. Karstens, D. Dobur, N.N. Vlasov

Fakultät für Physik der Universität Freiburg i.Br., Freiburg i.Br., Germany³³

M. Bell, P.J. Bussey, A.T. Doyle, J. Ferrando, J. Hamilton, S. Hanlon, D.H. Saxon,
I.O. Skillicorn

Department of Physics and Astronomy, University of Glasgow, Glasgow, United Kingdom⁴⁴

I. Gialas

Department of Engineering in Management and Finance, University of Aegean, Greece

T. Carli, T. Gosau, U. Holm, N. Krumnack, E. Lohrmann, M. Milite, H. Salehi,
P. Schleper, S. Stonjek¹¹, K. Wichmann, K. Wick, A. Ziegler, Ar. Ziegler

*Institute of Experimental Physics, Hamburg University, Hamburg, Germany*³³

C. Collins-Tooth, C. Foudas, R. Gonçalo¹⁴, K.R. Long, A.D. Tapper

*High Energy Nuclear Physics Group, Imperial College London, London, United Kingdom*⁴⁴

P. Cloth, D. Filges

Forschungszentrum Jülich, Institut für Kernphysik, Jülich, Germany

M. Kataoka¹⁵, K. Nagano, K. Tokushuku¹⁶, S. Yamada, Y. Yamazaki

*Institute of Particle and Nuclear Studies, KEK, Tsukuba, Japan*³⁷

A.N. Barakbaev, E.G. Boos, N.S. Pokrovskiy, B.O. Zhautykov

Institute of Physics and Technology of Ministry of Education and Science of Kazakhstan, Almaty, Kazakhstan

D. Son

*Center for High Energy Physics, Kyungpook National University, Daegu, South Korea*³⁸

K. Piotrkowski

Institut de Physique Nucléaire, Université Catholique de Louvain, Louvain-la-Neuve, Belgium

F. Barreiro, C. Glasman¹⁷, O. González, L. Labarga, J. del Peso, E. Tassi, J. Terrón,
M. Vázquez, M. Zambrana

*Departamento de Física Teórica, Universidad Autónoma de Madrid, Madrid, Spain*⁴³

M. Barbi, F. Corriveau, S. Gliga, J. Lainesse, S. Padhi, D.G. Stairs, R. Walsh

*Department of Physics, McGill University, Montréal, Québec, Canada H3A 2T8*³²

T. Tsurugai

*Faculty of General Education, Meiji Gakuin University, Yokohama, Japan*³⁷

A. Antonov, P. Danilov, B.A. Dolgoshein, D. Gladkov, V. Sosnovtsev, S. Suchkov

*Moscow Engineering Physics Institute, Moscow, Russia*⁴¹

R.K. Dementiev, P.F. Ermolov, Yu.A. Golubkov¹⁸, I.I. Katkov, L.A. Khein,
I.A. Korzhavina, V.A. Kuzmin, B.B. Levchenko¹⁹, O.Yu. Lukina, A.S. Proskuryakov,
L.M. Shcheglova, S.A. Zotkin

*Institute of Nuclear Physics, Moscow State University, Moscow, Russia*⁴²

N. Coppola, S. Grijpink, E. Koffeman, P. Kooijman, E. Maddox, A. Pellegrino,
S. Schagen, H. Tiecke, J.J. Velthuis, L. Wiggers, E. de Wolf

*NIKHEF and University of Amsterdam, Amsterdam, Netherlands*³⁹

N. Brümmer, B. Bylsma, L.S. Durkin, T.Y. Ling

*Physics Department, Ohio State University, Columbus, OH 43210, USA*⁴⁵

A.M. Cooper-Sarkar, A. Cottrell, R.C.E. Devenish, B. Foster, G. Grzelak,
C. Gwenlan²⁰, S. Patel, P.B. Straub, R. Walczak

*Department of Physics, University of Oxford, Oxford, United Kingdom*⁴⁴

A. Bertolin, R. Brugnera, R. Carlin, F. Dal Corso, S. Dusini, A. Garfagnini,
S. Limentani, A. Longhin, A. Parenti, M. Posocco, L. Stanco, M. Turcato

*Dipartimento di Fisica dell'Università and INFN, Padova, Italy*³⁶

E.A. Heaphy, F. Metlica, B.Y. Oh, J.J. Whitmore²¹

*Department of Physics, Pennsylvania State University, University Park, PA 16802, USA*⁴⁶

Y. Iga

*Polytechnic University, Sagamihara, Japan*³⁷

G. D'Agostini, G. Marini, A. Nigro

*Dipartimento di Fisica, Università 'La Sapienza' and INFN, Rome, Italy*³⁶

C. Cormack²², J.C. Hart, N.A. McCubbin

*Rutherford Appleton Laboratory, Chilton, Didcot, Oxon, United Kingdom*⁴⁴

C. Heusch

*University of California, Santa Cruz, CA 95064, USA*⁴⁵

I.H. Park

Department of Physics, Ewha Womans University, Seoul, South Korea

N. Pavel

Fachbereich Physik der Universität-Gesamthochschule Siegen, Germany

H. Abramowicz, A. Gabareen, S. Kananov, A. Kreisel, A. Levy

Raymond and Beverly Sackler Faculty of Exact Sciences, School of Physics, Tel-Aviv University, Tel-Aviv, Israel³⁵

M. Kuze

Department of Physics, Tokyo Institute of Technology, Tokyo, Japan³⁷

T. Fusayasu, S. Kagawa, T. Kohno, T. Tawara, T. Yamashita

Department of Physics, University of Tokyo, Tokyo, Japan³⁷

R. Hamatsu, T. Hirose², M. Inuzuka, H. Kaji, S. Kitamura²³, K. Matsuzawa

Department of Physics, Tokyo Metropolitan University, Tokyo, Japan³⁷

M.I. Ferrero, V. Monaco, R. Sacchi, A. Solano

Università di Torino and INFN, Torino, Italy³⁶

M. Arneodo, M. Ruspa

Università del Piemonte Orientale, Novara, and INFN, Torino, Italy³⁶

T. Koop, J.F. Martin, A. Mirea

Department of Physics, University of Toronto, Toronto, Ontario, Canada M5S 1A7³²

J.M. Butterworth²⁴, R. Hall-Wilton, T.W. Jones, M.S. Lightwood, M.R. Sutton⁴,
C. Targett-Adams

Physics and Astronomy Department, University College London, London, United Kingdom⁴⁴

J. Ciborowski²⁵, R. Ciesielski²⁶, P. Łuźniak²⁷, R.J. Nowak, J.M. Pawlak, J. Sztuk²⁸,
T. Tymieniecka²⁹, A. Ukleja²⁹, J. Ukleja³⁰, A.F. Żarnecki

Institute of Experimental Physics, Warsaw University, Warsaw, Poland⁴⁸

M. Adamus, P. Plucinski

Institute for Nuclear Studies, Warsaw, Poland⁴⁸

Y. Eisenberg, L.K. Gladilin³¹, D. Hochman, U. Karshon, M. Riveline

Department of Particle Physics, Weizmann Institute, Rehovot, Israel³⁴

D. Kçira, S. Lammers, L. Li, D.D. Reeder, M. Rosin, A.A. Savin, W.H. Smith

*Department of Physics, University of Wisconsin, Madison, WI 53706, USA*⁴⁵

A. Deshpande, S. Dhawan

*Department of Physics, Yale University, New Haven, CT 06520-8121, USA*⁴⁵

S. Bhadra, C.D. Catterall, S. Fourletov, G. Hartner, S. Menary, M. Soares, J. Standage

*Department of Physics, York University, Ontario, Canada M3J 1P3*³²

Received 19 January 2004; accepted 30 March 2004

Available online 8 May 2004

Editor: W.-D. Schlatter

Abstract

A search for physics beyond the Standard Model has been performed with high- Q^2 neutral current deep inelastic scattering events recorded with the ZEUS detector at HERA. Two data sets, $e^+p \rightarrow e^+X$ and $e^-p \rightarrow e^-X$, with respective integrated luminosities of 112 pb^{-1} and 16 pb^{-1} , were analyzed. The data reach Q^2 values as high as $40\,000 \text{ GeV}^2$. No significant deviations from Standard Model predictions were observed. Limits were derived on the effective mass scale in $eeqq$ contact interactions, the ratio of leptoquark mass to the Yukawa coupling for heavy leptoquark models and the mass scale parameter in models with large extra dimensions. The limit on the quark charge radius, in the classical form factor approximation, is $0.85 \times 10^{-16} \text{ cm}$.

© 2004 Published by Elsevier B.V. Open access under [CC BY license](#).

E-mail address: rik.yoshida@desy.de (R. Yoshida).

¹ Also affiliated with University College London, London, UK.

² Retired.

³ Self-employed.

⁴ PPARC Advanced Fellow.

⁵ Now at Dongshin University, Naju, South Korea.

⁶ Now at Max-Planck-Institut für Physik, München, Germany.

⁷ Partly supported by Polish Ministry of Scientific Research and Information Technology, Grant No. 2 P03B 122 25.

⁸ Partly supported by the Israel Science Foundation, and Ministry of Science, and Polish Ministry of Scientific Research and Information Technology, Grant No. 2 P03B 12625.

⁹ Supported by the Polish State Committee for Scientific Research, Grant No. 2 P03B 09322.

¹⁰ Now at DESY group FEE.

¹¹ Now at University of Oxford, Oxford, UK.

¹² On leave of absence at Columbia University, Nevis Labs., NY, USA.

¹³ Now at DESY group MPY.

¹⁴ Now at Royal Holloway University of London, London, UK.

¹⁵ Also at Nara Women's University, Nara, Japan.

¹⁶ Also at University of Tokyo, Tokyo, Japan.

¹⁷ Ramón y Cajal Fellow.

¹⁸ Now at HERA-B.

¹⁹ Partly supported by the Russian Foundation for Basic Research, Grant 02-02-81023.

²⁰ PPARC Postdoctoral Research Fellow.

²¹ On leave of absence at The National Science Foundation, Arlington, VA, USA.

²² Now at University of London, Queen Mary College, London, UK.

²³ Present address: Tokyo Metropolitan University of Health Sciences, Tokyo 116-8551, Japan.

²⁴ Also at University of Hamburg, Alexander von Humboldt Fellow.

²⁵ Also at Łódź University, Poland.

²⁶ Supported by the Polish State Committee for Scientific Research, Grant No. 2 P03B 07222.

²⁷ Łódź University, Poland.

²⁸ Łódź University, Poland, supported by the KBN Grant 2 P03B 12925.

²⁹ Supported by German Federal Ministry for Education and Research (BMBF), POL 01/043.

³⁰ Supported by the KBN Grant 2 P03B 12725.

1. Introduction

The HERA ep collider has extended the kinematic range of deep inelastic scattering (DIS) measurements by two orders of magnitude in Q^2 , the negative square of the four-momentum transfer, compared to fixed-target experiments. At values of Q^2 of about 4×10^4 GeV², the eq interaction, where q is a constituent quark of the proton, is probed at distances of $\sim 10^{-16}$ cm. Measurements in this domain allow searches for new physics processes with characteristic mass scales in the TeV range. New interac-

tions between e and q involving mass scales above the center-of-mass energy can modify the cross section at high Q^2 via virtual effects, resulting in observable deviations from the Standard Model (SM) predictions. Many such interactions, such as processes mediated by heavy leptoquarks, can be modelled as four-fermion contact interactions. The SM predictions for ep scattering in the Q^2 domain of this study result from the evolution of accurate measurements of the proton structure functions made at lower Q^2 . In this Letter, a common method is applied to search for four-fermion interactions, for graviton exchange in models with large extra dimensions, and for a finite charge radius of the quark.

In an analysis of 1994–1997 e^+p data [1], the ZEUS Collaboration set limits on the effective mass scale for the several parity-conserving compositeness models. Results presented here are based on approximately 130 pb^{-1} of e^+p and e^-p data collected by ZEUS in the years 1994–2000. Since this publication also includes the early ZEUS data, the results presented here supersede those of the earlier publication [1].

2. Standard Model cross section

The differential SM cross section for neutral current (NC) ep scattering, $e^\pm p \rightarrow e^\pm X$, can be expressed in terms of the kinematic variables Q^2 , x and y , which are defined by the four-momenta of the incoming electron⁴⁹ (k), the incoming proton (P), and the scattered electron (k') as $Q^2 = -q^2 = -(k - k')^2$, $x = Q^2/(2q \cdot P)$, and $y = (q \cdot P)/(k \cdot P)$. For unpolarized beams, the leading-order electroweak cross sections can be expressed as

$$\begin{aligned} \frac{d^2\sigma^{\text{NC}}(e^\pm p)}{dx dQ^2}(x, Q^2) \\ = \frac{2\pi\alpha^2}{xQ^4} \left[(1 + (1 - y)^2) F_2^{\text{NC}} \right. \\ \left. \mp (1 - (1 - y)^2) x F_3^{\text{NC}} \right], \end{aligned} \quad (1)$$

where α is the electromagnetic coupling constant. The contribution of the longitudinal structure function,

³¹ On leave from MSU, partly supported by University of Wisconsin via the US–Israel BSF.

³² Supported by the Natural Sciences and Engineering Research Council of Canada (NSERC).

³³ Supported by the German Federal Ministry for Education and Research (BMBF), under contract numbers HZ1GUA 2, HZ1GUB 0, HZ1PDA 5, HZ1VFA 5.

³⁴ Supported by the MINERVA Gesellschaft für Forschung GmbH, the Israel Science Foundation, the US–Israel Binational Science Foundation and the Benozio Center for High Energy Physics.

³⁵ Supported by the German–Israel Foundation and the Israel Science Foundation.

³⁶ Supported by the Italian National Institute for Nuclear Physics (INFN).

³⁷ Supported by the Japanese Ministry of Education, Culture, Sports, Science and Technology (MEXT) and its grants for Scientific Research.

³⁸ Supported by the Korean Ministry of Education and Korea Science and Engineering Foundation.

³⁹ Supported by the Netherlands Foundation for Research on Matter (FOM).

⁴⁰ Supported by the Polish State Committee for Scientific Research, Grant No. 620/E-77/SPB/DESY/P-03/DZ 117/2003-2005.

⁴¹ Partially supported by the German Federal Ministry for Education and Research (BMBF).

⁴² Partly supported by the Russian Ministry of Industry, Science and Technology through its grant for Scientific Research on High Energy Physics.

⁴³ Supported by the Spanish Ministry of Education and Science through funds provided by CICYT.

⁴⁴ Supported by the Particle Physics and Astronomy Research Council, UK.

⁴⁵ Supported by the US Department of Energy.

⁴⁶ Supported by the US National Science Foundation.

⁴⁷ Supported by the Polish State Committee for Scientific Research, Grant No. 112/E-356/SPUB/DESY/P-03/DZ 116/2003-2005, 2 P03B 13922.

⁴⁸ Supported by the Polish State Committee for Scientific Research, Grant No. 115/E-343/SPUB-M/DESY/P-03/DZ 121/2001-2002, 2 P03B 07022.

⁴⁹ Unless otherwise specified, ‘electron’ refers to both positron and electron.

$F_L(x, Q^2)$, is negligible at high Q^2 and is not taken into account in this analysis. At leading order (LO) in QCD, the structure functions F_2^{NC} and $x F_3^{\text{NC}}$ are given by

$$\begin{aligned} F_2^{\text{NC}}(x, Q^2) &= \sum_{q=u,d,s,c,b} A_q(Q^2)[xq(x, Q^2) + x\bar{q}(x, Q^2)], \\ x F_3^{\text{NC}}(x, Q^2) &= \sum_{q=u,d,s,c,b} B_q(Q^2)[xq(x, Q^2) - x\bar{q}(x, Q^2)], \end{aligned}$$

where $q(x, Q^2)$ and $\bar{q}(x, Q^2)$ are the parton densities for quarks and antiquarks. The functions A_q and B_q are defined as

$$\begin{aligned} A_q(Q^2) &= \frac{1}{2}[(V_q^L)^2 + (V_q^R)^2 + (A_q^L)^2 + (A_q^R)^2], \\ B_q(Q^2) &= (V_q^L)(A_q^L) - (V_q^R)(A_q^R), \end{aligned}$$

where the coefficient functions $V_q^{L,R}$ and $A_q^{L,R}$ are given by:

$$\begin{aligned} V_q^i &= Q_q - (v_e \pm a_e)v_q \chi_Z, \\ A_q^i &= -(v_e \pm a_e)a_q \chi_Z, \\ v_f &= T_f^3 - 2 \sin^2 \theta_W Q_f, \\ a_f &= T_f^3, \\ \chi_Z &= \frac{1}{4 \sin^2 \theta_W \cos^2 \theta_W} \frac{Q^2}{Q^2 + M_Z^2}. \end{aligned} \quad (2)$$

In Eq. (2), the superscript i denotes the left (L) or right (R) helicity projection of the lepton field; the plus (minus) sign in the definitions of V_q^i and A_q^i is appropriate for $i = L(R)$. The coefficients v_f and a_f are the SM vector and axial-vector coupling constants of an electron ($f = e$) or quark ($f = q$); Q_f and T_f^3 denote the fermion charge and third component of the weak isospin; M_Z and θ_W are the mass of the Z^0 and the electroweak mixing angle, respectively.

3. Models for new physics

3.1. General contact interactions

Four-fermion contact interactions (CI) represent an effective theory, which describes low-energy effects

due to physics at much higher energy scales. Such models would describe the effects of heavy leptons, additional heavy weak bosons, and electron or quark compositeness. The CI approach is not renormalizable and is only valid in the low-energy limit. As strong limits have already been placed on scalar and tensor contact interactions [2], only vector currents are considered here. They can be represented by additional terms in the Standard Model Lagrangian, viz.:

$$\mathcal{L}_{\text{CI}} = \sum_{\substack{i,j=L,R \\ q=u,d,s,c,b}} \eta_{ij}^{eq} (\bar{e}_i \gamma^\mu e_i) (\bar{q}_j \gamma_\mu q_j), \quad (3)$$

where the sum runs over electron and quark helicities and quark flavors. The couplings η_{ij}^{eq} describe the helicity and flavor structure of contact interactions. The CI Lagrangian (Eq. (3)) results in the following modification of the functions V_q^i and A_q^i of Eq. (2):

$$\begin{aligned} V_q^i &= Q_q - (v_e \pm a_e)v_q \chi_Z + \frac{Q^2}{2\alpha} (\eta_{iL}^{eq} + \eta_{iR}^{eq}), \\ A_q^i &= -(v_e \pm a_e)a_q \chi_Z + \frac{Q^2}{2\alpha} (\eta_{iL}^{eq} - \eta_{iR}^{eq}). \end{aligned}$$

It was assumed that all up-type quarks have the same contact-interaction couplings, and a similar assumption was made for down-type quarks:⁵⁰

$$\begin{aligned} \eta_{ij}^{eu} &= \eta_{ij}^{ec} = \eta_{ij}^{et}, \\ \eta_{ij}^{ed} &= \eta_{ij}^{es} = \eta_{ij}^{eb}, \end{aligned}$$

leading to eight independent couplings, η_{ij}^{eq} , with $q = u, d$. Due to the impracticality of setting limits in an eight-dimensional space, a set of representative scenarios was analyzed. Each scenario is defined by a set of eight coefficients, ϵ_{ij}^{eq} , each of which may take the values ± 1 or zero, and the compositeness scale Λ . The couplings are then defined by

$$\eta_{ij}^{eq} = \epsilon_{ij}^{eq} \frac{4\pi}{\Lambda^2}.$$

Note that models that differ in the overall sign of the coefficients ϵ_{ij}^{eq} are distinct because of the interference with the SM.

⁵⁰ The results depend very weakly on this assumption since heavy quarks make only a very small contribution to high- Q^2 cross sections. In most cases, the same mass-scale limits were obtained for CI scenarios where only first-generation quarks are considered. The largest difference between the obtained mass-scale limits is about 2%.

Table 1

Coupling structure $[\epsilon_{LL}, \epsilon_{LR}, \epsilon_{RL}, \epsilon_{RR}]$ of the compositeness models and the 95% C.L. limits on the compositeness scale, Λ , resulting from the ZEUS analysis of 1994–2000 $e^\pm p$ data. Each row of the table represents two scenarios corresponding to $\eta > 0$ (Λ^+) and $\eta < 0$ (Λ^-). The same coupling structure applies to d and u quarks, except for the models U1 to U6, for which the couplings for the d quarks are zero. Also shown are results obtained by the H1 Collaboration, the $p\bar{p}$ collider experiments DØ and CDF, and the LEP experiments ALEPH, L3 and OPAL. For the LEP experiments, limits derived from the channel $e^+e^- \rightarrow q\bar{q}$ are quoted

ZEUS 1994–2000 $e^\pm p$ 95% C.L. (TeV)		H1		DØ		CDF		ALEPH		L3		OPAL			
Coupling structure															
Model	$[\epsilon_{LL}, \epsilon_{LR}, \epsilon_{RL}, \epsilon_{RR}]$	Λ^-	Λ^+	Λ^-	Λ^+	Λ^-	Λ^+	Λ^-	Λ^+	Λ^-	Λ^+	Λ^-	Λ^+	Λ^-	Λ^+
LL	[+1, 0, 0, 0]	1.7	2.7	1.6	2.8	4.2	3.3	3.7	2.5	6.2	5.4	2.8	4.2	3.1	5.5
LR	[0, +1, 0, 0]	2.4	3.6	1.9	3.3	3.6	3.4	3.3	2.8	3.3	3.0	3.5	3.3	4.4	3.8
RL	[0, 0, +1, 0]	2.7	3.5	2.0	3.3	3.7	3.3	3.2	2.9	4.0	2.4	4.6	2.5	6.4	2.7
RR	[0, 0, 0, +1]	1.8	2.7	2.2	2.8	4.0	3.3	3.6	2.6	4.4	3.9	3.8	3.1	4.9	3.5
VV	[+1, +1, +1, +1]	6.2	5.4	5.5	5.3	6.1	4.9	5.2	3.5	7.1	6.4	5.5	4.2	7.2	4.7
AA	[+1, -1, -1, +1]	4.7	4.4	4.1	2.5	5.5	4.7	4.8	3.8	7.9	7.2	3.8	6.1	4.2	8.1
VA	[+1, -1, +1, -1]	3.3	3.2	3.0	2.9										
X1	[+1, -1, 0, 0]	3.6	2.6			4.5	3.9								
X2	[+1, 0, +1, 0]	3.9	4.0												
X3	[+1, 0, 0, +1]	3.7	3.6	3.9	3.7	5.1	4.2			7.4	6.7	3.7	4.4	4.4	5.4
X4	[0, +1, +1, 0]	5.1	4.8	4.4	4.4	4.4	3.9			4.5	2.9	5.2	3.1	7.1	3.4
X5	[0, +1, 0, +1]	4.0	4.0												
X6	[0, 0, +1, -1]	2.5	3.5			4.3	4.0								
U1	[+1, -1, 0, 0] ^{eu}	3.8	3.6												
U2	[+1, 0, +1, 0] ^{eu}	5.0	4.2												
U3	[+1, 0, 0, +1] ^{eu}	5.0	4.1									5.2	9.2		
U4	[0, +1, +1, 0] ^{eu}	5.8	4.8									3.2	2.3		
U5	[0, +1, 0, +1] ^{eu}	5.2	4.3												
U6	[0, 0, +1, -1] ^{eu}	2.8	3.4												

In this Letter, different chiral structures of CI are considered, as listed in Table 1. Models listed in the lower part of the table were previously considered in the published analysis of 1994–1997 e^+p data [1]. They fulfill the relation

$$\eta_{LL}^{eq} + \eta_{LR}^{eq} - \eta_{RL}^{eq} - \eta_{RR}^{eq} = 0,$$

which was imposed to conserve parity, and thereby complement strong limits from atomic parity violation (APV) results [3,4]. Since a later APV analysis [5] indicated possible deviations from SM predictions, models that violate parity, listed in the upper part of Table 1, have also been incorporated in the analysis. The reported 2.3σ deviation [5] from the SM was later reduced to around 1σ , after re-evaluation of some of the theoretical corrections [6,7].

3.2. Leptoquarks

Leptoquarks (LQ) appear in certain extensions of the SM that connect leptons and quarks; they carry

both lepton and baryon numbers and have spin 0 or 1. According to the general classification proposed by Buchmüller, Rückl and Wyler [8], there are 14 possible LQ states: seven scalar and seven vector.⁵¹ In the limit of heavy LQs ($M_{LQ} \gg \sqrt{s}$), the effect of s - and t -channel LQ exchange is equivalent to a vector-type $eeqq$ contact interaction.⁵² The effective contact-interaction couplings, η_{ij}^{eq} , are proportional to the square of the ratio of the leptoquark Yukawa coupling, λ_{LQ} , to the leptoquark mass, M_{LQ} :

$$\eta_{ij}^{eq} = a_{ij}^{eq} \left(\frac{\lambda_{LQ}}{M_{LQ}} \right)^2,$$

⁵¹ Leptoquark states are named according to the so-called Aachen notation [9].

⁵² For the invariant mass range accessible at HERA, $\sqrt{s} \sim 300$ GeV, heavy LQ approximation is applicable for $M_{LQ} > 400$ GeV. For ZEUS limits covering LQ masses below 400 GeV see [10].

Table 2

Coefficients a_{ij}^{eq} defining the effective leptoquark couplings in the contact-interaction limit $M_{LQ} \gg \sqrt{s}$ and the 95% C.L. lower limits on the leptoquark mass to the Yukawa coupling ratio M_{LQ}/λ_{LQ} resulting from the CI analysis of the ZEUS 1994–2000 $e^\pm p$ data, for different models of scalar (upper part of the table) and vector (lower part) leptoquarks. Also shown are results obtained by the H1 Collaboration and corresponding contact-interaction limits from the LEP experiments L3 and OPAL. The limits from LEP on the compositeness scale Λ , for models with coupling structure corresponding to those of scalar (vector) leptoquarks, were scaled by factor $1/\sqrt{8\pi}$ ($1/\sqrt{4\pi}$)

ZEUS 1994–2000 $e^\pm p$ 95% C.L.			M_{LQ}/λ_{LQ} (TeV)		
Model	Coupling structure	M_{LQ}/λ_{LQ} (TeV)	H1	L3	OPAL
S_0^L	$a_{LL}^{eu} = +\frac{1}{2}$	0.61	0.71	1.40	0.98
S_0^R	$a_{RR}^{eu} = +\frac{1}{2}$	0.56	0.64	0.30	0.30
\tilde{S}_0^R	$a_{RR}^{ed} = +\frac{1}{2}$	0.27	0.33	0.58	0.80
$S_{1/2}^L$	$a_{LR}^{eu} = -\frac{1}{2}$	0.83	0.85	0.54	0.74
$S_{1/2}^R$	$a_{RL}^{ed} = a_{RL}^{eu} = -\frac{1}{2}$	0.53	0.37		0.86
$\tilde{S}_{1/2}^L$	$a_{LR}^{ed} = -\frac{1}{2}$	0.43	0.43	0.42	0.48
S_1^L	$a_{LL}^{ed} = +1, a_{LL}^{eu} = +\frac{1}{2}$	0.52	0.49		
V_0^L	$a_{LL}^{ed} = -1$	0.55	0.73	1.83	1.27
V_0^R	$a_{RR}^{ed} = -1$	0.47	0.58	0.51	0.54
\tilde{V}_0^R	$a_{RR}^{eu} = -1$	0.87	0.99	1.02	1.44
$V_{1/2}^L$	$a_{LR}^{ed} = +1$	0.47	0.42	0.71	0.90
$V_{1/2}^R$	$a_{RL}^{ed} = a_{RL}^{eu} = +1$	0.99	0.95		0.71
$\tilde{V}_{1/2}^L$	$a_{LR}^{eu} = +1$	1.06	1.02	0.54	0.59
V_1^L	$a_{LL}^{ed} = -1, a_{LL}^{eu} = -2$	1.23	1.36		

where the coefficients a_{ij}^{eq} depend on the LQ species [11] and are twice as large for vector as for scalar leptoquarks. Only first-generation leptoquarks are considered in this analysis, $q = u, d$. The coupling structure for different leptoquark species is shown in Table 2. Leptoquark models S_0^L and $\tilde{S}_{1/2}^L$ correspond to the squark states \tilde{d}_R and \tilde{u}_L , in minimal supersymmetric theories with broken R -parity.

3.3. Large extra dimensions

Arkani-Hamed, Dimopoulos and Dvali [12–14] have proposed a model to solve the hierarchy problem, assuming that space–time has $4 + n$ dimensions. Particles, including strong and electroweak bosons, are confined to four dimensions, but gravity can propagate into the extra dimensions. The extra n spatial dimensions are compactified with a radius R . The Planck scale, $M_P \sim 10^{19}$ GeV, in 4 dimensions is an effective scale arising from the fundamental Planck

scale M_D in $D = 4 + n$ dimensions. The two scales are related by:

$$M_P^2 \sim R^n M_D^{2+n}.$$

For extra dimensions with $R \sim 1$ mm for $n = 2$, the scale M_D can be of the order of TeV. At high energies, the strengths of the gravitational and electroweak interactions can then become comparable. After summing the effects of graviton excitations in the extra dimensions, the graviton-exchange contribution to $eq \rightarrow eq$ scattering can be described as a contact interaction with an effective coupling strength of [15,16]

$$\eta_G = \frac{\lambda}{M_S^4},$$

where M_S is an ultraviolet cutoff scale, expected to be of the order of M_D , and the coupling λ is of order unity. Since the sign of λ is not known a priori, both values $\lambda = \pm 1$ are considered in this analysis. However, due to additional energy-scale dependence,

reflecting the number of accessible graviton excitations, these contact interactions are not equivalent to the vector contact interactions of Eq. (3). To describe the effects of graviton exchange, terms arising from pure graviton exchange (G), graviton–photon interference (γG) and graviton- Z (ZG) interference have to be added to the SM $eq \rightarrow eq$ scattering cross section [17]:

$$\begin{aligned} \frac{d\sigma(e^\pm q \rightarrow e^\pm q)}{d\hat{t}} &= \frac{d\sigma^{\text{SM}}}{d\hat{t}} + \frac{d\sigma^G}{d\hat{t}} + \frac{d\sigma^{\gamma G}}{d\hat{t}} + \frac{d\sigma^{ZG}}{d\hat{t}}, \\ \frac{d\sigma^G}{d\hat{t}} &= \frac{\pi\lambda^2}{32M_S^8 \hat{s}^2} \{32\hat{u}^4 + 64\hat{u}^3\hat{t} \\ &\quad + 42\hat{u}^2\hat{t}^2 + 10\hat{u}\hat{t}^3 + \hat{t}^4\}, \\ \frac{d\sigma^{\gamma G}}{d\hat{t}} &= \mp \frac{\pi\lambda}{2M_S^4 \hat{s}^2} \frac{\alpha Q_q}{\hat{t}} (2\hat{u} + \hat{t})^3, \\ \frac{d\sigma^{ZG}}{d\hat{t}} &= \frac{\pi\lambda}{2M_S^4 \hat{s}^2 \sin^2 2\theta_W} \left\{ \pm v_e v_q \frac{(2\hat{u} + \hat{t})^3}{\hat{t} - M_Z^2} \right. \\ &\quad \left. - a_e a_q \frac{\hat{t}(6\hat{u}^2 + 6\hat{u}\hat{t} + \hat{t}^2)^3}{\hat{t} - M_Z^2} \right\}, \end{aligned}$$

where \hat{s} , \hat{t} and \hat{u} , with $\hat{t} = -Q^2$, are the Mandelstam variables, while the other coefficients are given in Eq. (2). The corresponding cross sections for $e^\pm \bar{q}$ scattering are obtained by changing the sign of Q_q and v_q parameters.

Graviton exchange also contributes to electron–gluon scattering, $eg \rightarrow eg$, which is not present at leading order in the SM:

$$\begin{aligned} \frac{d\sigma(e^\pm g \rightarrow e^\pm g)}{d\hat{t}} &= \frac{\pi\lambda^2}{2M_S^8 \hat{s}^2} \{2\hat{u}^3 + 4\hat{u}^2\hat{t} + 3\hat{u}\hat{t}^2 + \hat{t}^3\}. \end{aligned}$$

For a given point in the (x, Q^2) plane, the $e^\pm p$ cross section is then given by

$$\begin{aligned} \frac{d^2\sigma(e^\pm p \rightarrow e^\pm X)}{dx dQ^2}(x, Q^2) &= q(x, Q^2) \frac{d\sigma(e^\pm q)}{d\hat{t}} q(x, Q^2) \frac{d\sigma(e^\pm \bar{q})}{d\hat{t}} \\ &\quad + g(x, Q^2) \frac{d\sigma(e^\pm g)}{d\hat{t}}, \end{aligned}$$

where $q(x, Q^2)$, $\bar{q}(x, Q^2)$ and $g(x, Q^2)$ are the quark, antiquark and gluon densities in the proton, respectively.

3.4. Quark form factor

Quark substructure can be detected by measuring the spatial distribution of the quark charge. If $Q^2 \ll 1/R_e^2$ and $Q^2 \ll 1/R_q^2$, the SM predictions for the cross sections are modified, approximately, to:

$$\frac{d\sigma}{dQ^2} = \frac{d\sigma^{\text{SM}}}{dQ^2} \left(1 - \frac{R_e^2}{6} Q^2\right)^2 \left(1 - \frac{R_q^2}{6} Q^2\right)^2,$$

where R_e and R_q are the root-mean-square radii of the electroweak charge of the electron and the quark, respectively.

4. Data samples

The data used in this analysis were collected with the ZEUS detector at HERA and correspond to an integrated luminosity of 48 pb⁻¹ and 63 pb⁻¹ for e^+p collisions collected in 1994–1997 and 1999–2000, respectively, and 16 pb⁻¹ for e^-p collisions collected in 1998–1999. The 1994–1997 data set was collected at $\sqrt{s} = 300$ GeV and the 1998–2000 data sets were taken with $\sqrt{s} = 318$ GeV.

The analysis is based upon the final event samples used in previously published cross section measurements [18–20]. Only events with $Q^2 > 1000$ GeV² are considered. The SM predictions were taken from the simulated event samples used in the cross section measurements, where selection cuts and event reconstruction are identical to those applied to the data. Neutral current DIS events were simulated using the HERACLES [21] program with DJANGO [22, 23] for electroweak radiative corrections and higher-order matrix elements, and the color-dipole model of ARIADNE [24] for the QCD cascade and hadronization. The ZEUS detector was simulated using a program based on GEANT 3.13 [25]. The details of the data selection and reconstruction, and the simulation used can be found elsewhere [18–20].

The distributions of NC DIS events in Q^2 , measured separately for each of the three data sets, are in good agreement with SM predictions calculated using the CTEQ5D parameterization [26,27] of the par-

ton distribution functions (PDFs) of the proton. The CTEQ5D parameterization is based on a global QCD analysis of the data on high energy lepton–hadron and hadron–hadron interactions, including high- Q^2 H1 and ZEUS results based on the 1994 e^+p data. The ZEUS data used in the CTEQ analysis amount to less than 3% of the sample considered in this analysis. In general, SM predictions in the Q^2 range considered here are dominantly determined by fixed-target data at $Q^2 < 100 \text{ GeV}^2$ and $x > 0.01$ [28].

5. Analysis method

5.1. Monte Carlo reweighting

The contact interactions analysis was based on a comparison of the measured Q^2 distributions with the predictions of the MC simulation. The effects of each CI scenario are taken into account by reweighting each MC event of the type $ep \rightarrow eX$ with the weight

$$w = \frac{\frac{d^2\sigma}{dx dQ^2}(\text{SM} + \text{CI})}{\frac{d^2\sigma}{dx dQ^2}(\text{SM})} \Bigg|_{\text{true } x, Q^2} \quad (4)$$

The weight w was calculated as the ratio of the leading-order⁵³ cross sections, Eq. (1), evaluated at the true values of x and Q^2 as determined from the four-momenta of the exchanged boson and the incident particles. In simulated events where a photon with energy E_γ is radiated by the incoming electron (initial-state radiation), the electron energy is reduced by E_γ . This approach guarantees that possible differences between the SM and the CI model in event-selection efficiency and migration corrections are properly taken into account. Under the assumption that the difference between the SM predictions and those of the model including contact interactions is small, higher-order QCD and electroweak corrections, including radiative corrections, are also accounted for.

5.2. Limit-setting procedure

For each of the models of new physics described above, it is possible to characterize the strength of the

interaction by a single parameter: $4\pi/\Lambda^2$ for contact interactions; $(\lambda_{\text{LQ}}/M_{\text{LQ}})^2$ for leptoquarks; λ/M_S^4 for models with large extra dimensions; and R_q^2 for the quark form factor. In the following, this parameter is denoted by η . For contact interactions, models with large extra dimensions and the quark form factor model, scenarios with positive and negative η values were considered separately.

For a given model, the likelihood was calculated as

$$L(\eta) = \prod_i e^{-\mu_i(\eta)} \cdot \frac{\mu_i(\eta)^{n_i}}{n_i!},$$

where the product runs over all Q^2 bins, n_i is the number of events observed in Q^2 bin i and $\mu_i(\eta)$ is the expected number of events in that bin for a coupling strength η . The likelihood for the complete $e^\pm p$ data set was obtained by multiplying the likelihoods for each of the three running periods.

The value of η for which $L(\eta)$ is maximized is denoted as η_0 . First η_0^{data} , the value of η that best describes the observed Q^2 spectra was determined. Using ensembles of Monte Carlo experiments (MCE), the expected distribution of η_0 was then determined as a function of η_{MC} the coupling value used as the input to the simulation. The 95% C.L. limit on η was defined as the value of η_{MC} for which the probability that $|\eta_0| > |\eta_0^{\text{data}}|$ was 0.95.

For each value of η_{MC} , the nominal number of events expected in each Q^2 bin i , denoted $\tilde{\mu}_i(\eta_{\text{MC}})$ was calculated by reweighting the SM MC prediction according to Eq. (4). Theoretical and experimental systematic uncertainties were taken into account by treating each uncertain quantity as a random variable. For each uncertainty, 100% correlation between systematic variations in different bins was assumed. For each individual MCE, an independent random variable, δ_j , with zero mean, was generated for each systematic uncertainty j . The expected number of events in each Q^2 bin i was then given by the product of the nominal expectation, $\tilde{\mu}_i$, and N_{sys} random factors which account for the uncertainties in the estimation of μ_i as follows:

$$\mu_i = \tilde{\mu}_i(\eta_{\text{MC}}) \cdot \prod_{j=1}^{N_{\text{sys}}} (1 + c_{ij})^{\delta_j}.$$

The coefficient c_{ij} is the fractional change in the expected number of events in bin i for a unit change

⁵³ Note that CIs constitute a non-renormalizable effective theory for which higher orders are not well defined.

in δ_j . This definition of μ_i reduces to a linear dependence of μ_i on each δ_j when δ_j is small, while avoiding the possibility of μ_i becoming negative which would arise if μ_i was defined as a linear function of the δ_j 's. For most of the systematic uncertainties, δ_j follows a Gaussian distribution, except for a few where it follows a uniform distribution, as noted in the next section. For a Gaussian δ_j distribution, the definition of μ_i corresponds to a Gaussian distribution in $\log \mu_i$. About one million MCEs were generated for each model, so that the statistical error was negligible.

5.3. Systematic uncertainties

Uncertainties in the SM cross sections considered in this study were estimated using the EPDFLIB program [29] based on QCDNUM [30]. Fractional variations estimated from EPDFLIB were used to rescale the nominal SM expectations calculated with CTEQ5D. The following uncertainties were included:

- statistical and systematic uncertainties of the data used as an input to the NLO QCD fit. These errors were the largest uncertainty in the SM expectations. At high Q^2 , the uncertainty is up to about 4.5% (3%) for e^+p (e^-p) data;
- uncertainty in the value of $\alpha_S(M_Z^2)$ used in the NLO QCD fit. The resulting uncertainties of NC DIS cross sections at high Q^2 , estimated assuming an error on $\alpha_S(M_Z^2)$ of ± 0.002 [31], is about 1.6%;
- uncertainties in the nuclear corrections applied to the deuteron data (K_D) and to the data from neutrino scattering on iron (K_{Fe}) used in QCDNUM. As suggested in EPDFLIB, variations by up to 100% for K_D and 50% for K_{Fe} were applied, treating the corrections as uniformly distributed random variables. The corresponding uncertainties of NC DIS cross sections at high Q^2 , are up to about 1.7% (0.8%) for K_D and up to about 3% (0.7%) for K_{Fe} , for e^+p (e^-p) data.

The PDF uncertainties calculated using EPDFLIB are similar to those obtained from a ZEUS NLO QCD fit [28], when high- Q^2 HERA data were excluded from the fit.

In addition to the uncertainty in the SM prediction, the following experimental uncertainties were taken into account:

- the scale uncertainty on the energy of the scattered electron of $\pm(1-3)\%$ depending on the topology of the event [32]. The resulting uncertainty of NC DIS cross section at high Q^2 is about 0.6% (1.3%), for e^+p (e^-p) data;
- the uncertainty in the hadronic energy scale of $\pm(1-2)\%$ depending on the topology of the event [33]. The resulting cross section uncertainty at high Q^2 is about 1%, for both e^+p and e^-p data;
- uncertainties on the luminosity measurement of 1.6% for the 1994–1997 e^+p data, 1.8% for the 1998–1999 e^-p data and 2.5% for the 1999–2000 e^+p data. Correlations between luminosity uncertainties for different data-taking periods are small and were neglected in the analysis.

As the double-angle method used to reconstruct the kinematics of the events [18–20] is relatively insensitive to uncertainties in the absolute energy scale of the calorimeter, the largest experimental uncertainty in the numbers of NC DIS events expected at high Q^2 is due to the luminosity measurement.

6. Results

No significant deviation of the ZEUS data from the SM prediction using the CTEQ5D parameterization of the proton PDF was observed. For all models considered, the best description of the data was obtained for very small values of $|\eta_0^{\text{data}}|$, i.e., close to the SM. The probability of obtaining larger best-fit coupling from the SM, i.e., the probability that an experiment would produce a value of $|\eta_0|$ greater than that obtained from the data, $|\eta_0| > |\eta_0^{\text{data}}|$, calculated with MCEs assuming the SM cross section, was above 25% in all cases. Therefore, limits on the strength parameters of the models described in Section 3 are presented in this Letter.

The measured Q^2 spectra for e^+p and e^-p data, normalized to the SM predictions are shown in Fig. 1. Also shown are curves, for VV and AA contact-interaction models (Section 3.1), which correspond to the 95% C.L. exclusion limits on Λ . The 95% C.L.

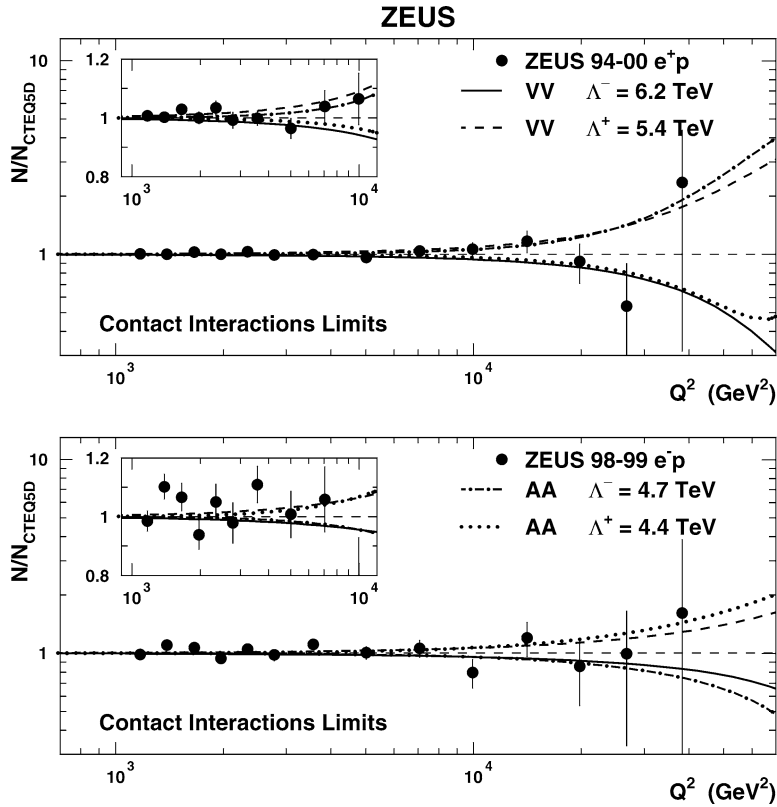


Fig. 1. ZEUS data compared with 95% C.L. exclusion limits for the effective mass scale in the VV and AA contact-interaction models, for positive (Λ^+) and negative (Λ^-) couplings. Results are normalized to the Standard Model expectations calculated using the CTEQ5D parton distributions. The insets show the comparison in the $Q^2 < 10^4$ GeV² region, with a linear ordinate scale.

limits on the compositeness scale Λ , for different CI models, are compared in Fig. 2 and Table 1. Limits range from 1.7 TeV for the LL model to 6.2 TeV for the VV model. Also indicated in the figure are the best-fit coupling values, $\eta_0^{\text{data}} = \frac{4\pi}{\Lambda^2}$, for positive and negative couplings. For comparison, the positions of the global likelihood maxima with $\pm 1\sigma$ and $\pm 2\sigma$ error⁵⁴ bars are included in Fig. 2. Systematic uncertainties are taken into account by averaging the likelihood values over systematic uncertainties. For most models, the $\pm 2\sigma$ error bars are in good agreement with 95% C.L. limits calculated with the MCE approach.

⁵⁴ Errors are calculated from the likelihood variation: $\pm 1\sigma$ and $\pm 2\sigma$ errors correspond to the decrease of the likelihood value to $\log L(\eta) = \log L(\eta_0) - \frac{1}{2}$ and $\log L(\eta) = \log L(\eta_0) - 2$, respectively.

The 95% C.L. lower limits on the compositeness scale Λ are compared in Table 1 with limits from the H1 Collaboration [34], the Tevatron [35,36] and the LEP [37–40] experiments (where only the results from $e^+e^- \rightarrow q\bar{q}$ channel are quoted). In Table 1 the relations between CI couplings for the compositeness models considered are also included. The results on the compositeness scale Λ presented here are comparable to those obtained by other experiments, where they exist. For many models, this analysis sets the only existing limits.

The leptoquark analysis takes into account LQs that couple to the electron and the first-generation quarks (u, d) only (Section 3.2). Deviations in the Q^2 distribution of e^+p and e^-p NC DIS events, corresponding to the 95% C.L. exclusion limits for selected scalar and vector leptoquark models, are compared with ZEUS data in Fig. 3. The 95% C.L. limits on the ratio of the

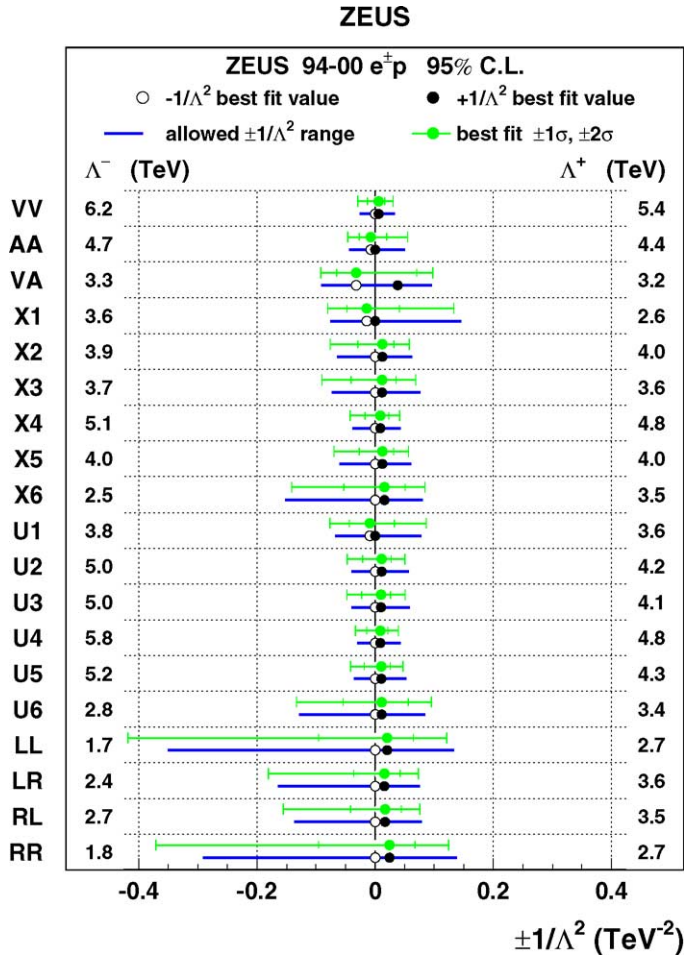


Fig. 2. Confidence intervals of $\pm 1/\Lambda^2$ at 95% C.L. for general CI scenarios studied in this Letter (dark horizontal bars). The numbers at the right (left) margin are the corresponding lower limits on the mass scale Λ^+ (Λ^-). The dark filled (open) circles indicate the positions corresponding to the best-fit coupling values, η_0^{data} , for positive (negative) couplings. The light filled circles with error bars indicate the position of the global likelihood maximum. For calculation of $\pm 1\sigma$ and $\pm 2\sigma$ errors on the global maximum position, likelihood values are averaged over systematic uncertainties.

leptoquark mass to the Yukawa coupling, $M_{\text{LQ}}/\lambda_{\text{LQ}}$, are summarized in Table 2 together with the coefficients a_{ij}^{eq} describing the CI coupling structure. The limits range from 0.27 TeV for \tilde{S}_0^R model to 1.23 TeV for V_1^L model. Table 2 also shows the LQ limits obtained by the H1 Collaboration [34] and by the LEP experiments [37,39]. In general, comparable limits are obtained. For the S_1^L , $V_{1/2}^R$ and $\tilde{V}_{1/2}^L$ leptoquarks, the ZEUS analysis provides the most stringent limits.

When only the NC DIS event sample is considered, the leptoquark limits obtained in the contact-interaction approximation are similar to, or better than,

the high-mass limits from the ZEUS resonance-search analysis [10]. However, for S_0^L , S_1^L and V_0^L models these previously published limits are more stringent, as the possible leptoquark contribution to charged current DIS was also taken into account.

For the model with large extra dimensions (Section 3.3), 95% C.L. lower limits on the mass scale in n dimensions of

$$M_S > 0.78 \text{ TeV} \quad \text{for } \lambda = +1,$$

$$M_S > 0.79 \text{ TeV} \quad \text{for } \lambda = -1,$$

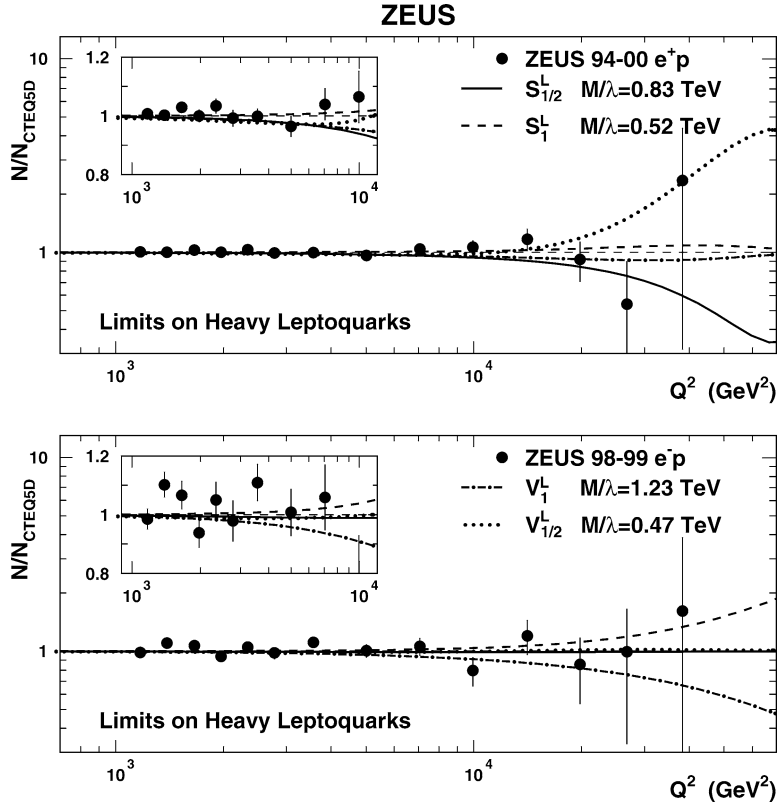


Fig. 3. ZEUS data compared with 95% C.L. exclusion limits for the ratio of the leptoquark mass to the Yukawa coupling, M/λ , for the $S_{1/2}^L$, S_1^L , V_1^L and $V_{1/2}^L$ leptoquarks. Results are normalized to the Standard Model expectations calculated using the CTEQ5D parton distributions. The insets show the comparison in the $Q^2 < 10^4$ GeV^2 region, with a linear ordinate scale.

were obtained. In Fig. 4, effects of graviton exchange on the Q^2 distribution, corresponding to these limits, are compared with ZEUS e^+p (Fig. 4(a)) and e^-p (Fig. 4(b)) data. The limits on M_S obtained in this analysis are similar to those obtained by the H1 Collaboration [34] and stronger than limits from $q\bar{q}$ production at LEP [41]. However, if all final states are considered, the limits derived from e^+e^- collisions exceed 1 TeV [41]. Limits above 1 TeV are also obtained in $p\bar{p}$ from the measurement of e^-e^+ and $\gamma\gamma$ production [42].

Assuming the electron to be point-like ($R_e = 0$), the 95% C.L. upper limit on the effective quark-charge radius (Section 3.4) of

$$R_q < 0.85 \times 10^{-16} \text{ cm}$$

was obtained. The present result improves the limits set in ep scattering by the H1 Collaboration [34]

($R_q < 1.0 \times 10^{-16}$ cm) and is similar to the limit set by the CDF Collaboration in $p\bar{p}$ collisions using the Drell–Yan production of e^+e^- and $\mu^+\mu^-$ pairs [35] ($R_q < 0.79 \times 10^{-16}$ cm).⁵⁵ The L3 Collaboration has presented a stronger limit ($R_q < 0.42 \times 10^{-16}$ cm, assuming $R_e = 0$), based on quark-pair production measurement at LEP2 [39] and assuming the same effective charge radius for all produced quark flavors.

If the charge distribution in the quark changes sign as a function of the radius, negative values can also be considered for R_q^2 . For such a model, the ZEUS 95%

⁵⁵ Limits on the effective quark radius published by the CDF Collaboration [35] were calculated assuming $R_q = R_e$. For comparison with limits assuming $R_e = 0$, the limit value was scaled by a factor $\sqrt{2}$.

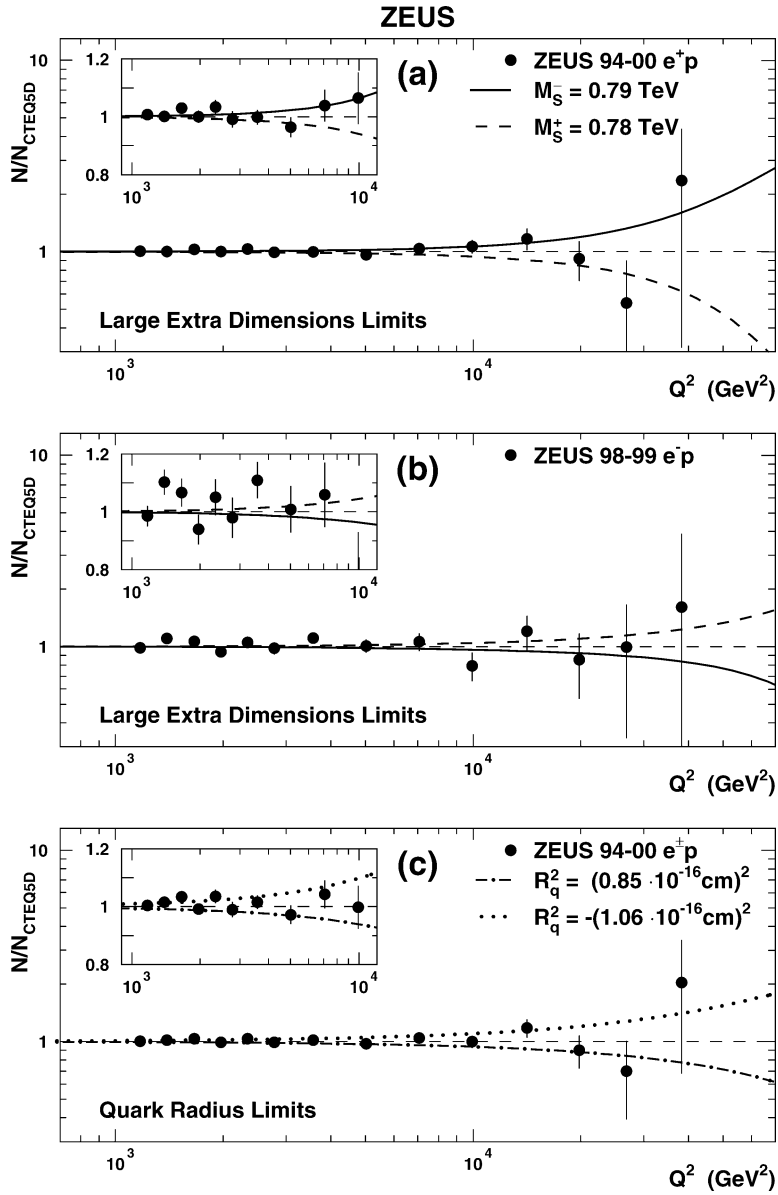


Fig. 4. ZEUS e^+p data (a) and e^-p data (b) compared with 95% C.L. exclusion limits for the effective Planck mass scale in models with large extra dimensions, for positive (M_S^+) and negative (M_S^-) couplings. (c) Combined 1994–2000 data compared with 95% C.L. exclusion limits for the effective mean-square radius of the electroweak charge of the quark. Results are normalized to the Standard Model expectations calculated using the CTEQ5D parton distributions. The insets show the comparison in the $Q^2 < 10^4$ GeV² region, with a linear ordinate scale.

C.L. upper limit on the effective quark-charge radius squared can be written as:

$$-R_q^2 < (1.06 \times 10^{-16} \text{ cm})^2.$$

Cross section deviations corresponding to the 95% C.L. exclusion limits for the effective radius, R_q , of the electroweak charge of the quark are compared with the ZEUS data in Fig. 4(c).

7. Conclusions

A search for signatures of physics beyond the Standard Model has been performed with the e^+p and e^-p data collected by the ZEUS Collaboration in the years 1994–2000, with integrated luminosities of 112 and 16 pb⁻¹, reaching Q^2 values as high as 4×10^4 GeV². No significant deviation from Standard Model predictions was observed and 95% C.L. limits were obtained for the relevant parameters of the models studied. For the contact-interaction models, limits on the effective mass scale, Λ (i.e., compositeness scale), ranging from 1.7 to 6.2 TeV have been obtained. Limits ranging from 0.27 to 1.23 TeV have been set for the ratio of the leptoquark mass to the Yukawa coupling, M_{LQ}/λ_{LQ} , in the limit of large leptoquark masses, $M_{LQ} \gg \sqrt{s}$. Limits were derived on the mass scale parameter in models with large extra dimensions: for positive (negative) coupling signs, scales below 0.78 TeV (0.79 TeV) are excluded. A quark-charge radius larger than 0.85×10^{-16} cm has been excluded, using the classical form-factor approximation.

The limits derived in this analysis are comparable to the limits obtained by the H1 Collaboration and by the LEP and Tevatron experiments. For many models the analysis presented here provides the most stringent limits to date.

Acknowledgements

This measurement was made possible by the inventiveness and the diligent efforts of the HERA machine group. The strong support and encouragement of the DESY directorate has been invaluable. The design, construction, and installation of the ZEUS detector has been made possible by the ingenuity and dedicated effort of many people who are not listed as authors. Their contributions are acknowledged with great appreciation.

References

- [1] ZEUS Collaboration, J. Breitweg, et al., Eur. Phys. J. C 14 (2000) 239.
- [2] P. Haberl, F. Schrempp, H.U. Martyn, in: W. Buchmüller, G. Ingelman (Eds.), Proceedings of Workshop on Physics at HERA, Hamburg, Germany, 1991, p. 1133.
- [3] C.S. Wood, et al., Science 275 (1997) 1759.
- [4] S.A. Blundell, J. Sapirstein, W.R. Johnson, Phys. Rev. D 45 (1992) 1602.
- [5] S.C. Bennett, C.E. Wieman, Phys. Rev. Lett. 82 (1999) 2484.
- [6] A. Derevianko, Phys. Rev. Lett. 85 (2000) 1618.
- [7] M.G. Kozlov, S.G. Porsev, I.I. Tupitsyn, Phys. Rev. Lett. 86 (2001) 3260.
- [8] W. Buchmüller, R. Rückl, D. Wyler, Phys. Lett. B 191 (1987) 442; W. Buchmüller, R. Rückl, D. Wyler, Phys. Lett. B 448 (1999) 320, Erratum.
- [9] A. Djouadi, et al., Z. Phys. C 46 (1990) 679.
- [10] ZEUS Collaboration, S. Chekanov, et al., Phys. Rev. D 68 (2003) 052004.
- [11] J. Kalinowski, et al., Z. Phys. C 74 (1997) 595.
- [12] N. Arkani-Hamed, S. Dimopoulos, G. Dvali, Phys. Lett. B 429 (1998) 263.
- [13] I. Antoniadis, et al., Phys. Lett. B 436 (1998) 257.
- [14] N. Arkani-Hamed, S. Dimopoulos, G. Dvali, Phys. Rev. D 59 (1999) 086004.
- [15] G.F. Giudice, R. Rattazzi, J.D. Wells, Nucl. Phys. B 544 (1999) 3.
- [16] K. Cheung, Phys. Lett. B 460 (1999) 383.
- [17] H1 Collaboration, C. Adloff, et al., Phys. Lett. B 479 (2000) 358.
- [18] ZEUS Collaboration, J. Breitweg, et al., Eur. Phys. J. C 11 (1999) 427.
- [19] ZEUS Collaboration, S. Chekanov, et al., Eur. Phys. J. C 28 (2003) 175.
- [20] ZEUS Collaboration, S. Chekanov, et al., Preprint DESY-03-214, hep-ex/0401003, Phys. Rev. D (2003), submitted for publication.
- [21] A. Kwiatkowski, H. Spiesberger, H.-J. Möhring, Comput. Phys. Commun. 69 (1992) 155; Also A. Kwiatkowski, H. Spiesberger, H.-J. Möhring, in: W. Buchmüller, G. Ingelman (Eds.), Proceedings of Workshop on Physics at HERA, Hamburg, Germany, 1991, p. 1294.
- [22] K. Charchula, G.A. Schuler, H. Spiesberger, Comput. Phys. Commun. 81 (1994) 381.
- [23] H. Spiesberger, HERACLES and DJANGO: Event Generation for ep Interactions at HERA Including Radiative Processes, 1998, available on <http://www.desy.de/~hspiesb/djangoh.html>.
- [24] L. Lönnblad, Comput. Phys. Commun. 71 (1992) 15.
- [25] R. Brun, et al., GEANT3, Technical report CERN-DD/EE/84-1, CERN, 1987.
- [26] CTEQ Collaboration, H.L. Lai, et al., Eur. Phys. J. C 12 (2000) 375.
- [27] H.L. Lai, et al., Phys. Rev. D 55 (1997) 1280.
- [28] ZEUS Collaboration, S. Chekanov, et al., Phys. Rev. D 67 (2003) 012007.
- [29] M. Botje, Fast access to parton densities, errors and correlations, EPDFLIB v. 2.0. NIKHEF-99-034.
- [30] M. Botje, Eur. Phys. J. C 14 (2000) 285.

- [31] Particle Data Group, K. Hagiwara, et al., *Phys. Rev. D* 66 (2002) 010001.
- [32] ZEUS Collaboration, S. Chekanov, et al., *Eur. Phys. J. C* 21 (2001) 443.
- [33] ZEUS Collaboration, S. Chekanov, et al., *Phys. Lett. B* 539 (2002) 197.
- [34] H1 Collaboration, C. Adloff, et al., *Phys. Lett. B* 568 (2003) 35.
- [35] CDF Collaboration, F. Abe, et al., *Phys. Rev. Lett.* 79 (1997) 2198.
- [36] DØ Collaboration, B. Abbott, et al., *Phys. Rev. Lett.* 82 (1999) 4769.
- [37] ALEPH Collaboration, R. Barate, et al., *Eur. Phys. J. C* 12 (2000) 183.
- [38] DELPHI Collaboration, P. Abreu, et al., *Eur. Phys. J. C* 11 (1999) 383.
- [39] L3 Collaboration, M. Acciarri, et al., *Phys. Lett. B* 489 (2000) 81.
- [40] OPAL Collaboration, G. Abbiendi, et al., *Eur. Phys. J. C* 13 (2000) 553.
- [41] L3 Collaboration, M. Acciarri, et al., *Phys. Lett. B* 470 (1999) 281.
- [42] DØ Collaboration, D. Abbott, et al., *Phys. Rev. Lett.* 86 (2001) 1156.